Histochem Cell Biol (2010) 133:527–539
DOI 10.1007/s00418-010-0690-1

ORIGINAL PAPER

Prominin-2 is a novel marker of distal tubules and collecting ducts of the human and murine kidney

József Jászai · Lilla M. Farkas · Christine A. Fargeas · Peggy Janich · Michael Haase · Wieland B. Huttner · Denis Corbeil

Accepted: 6 March 2010 / Published online: 24 March 2010

Abstract Prominin-1 (CD133) and its paralogue, prominin-2, are pentaspan membrane glycoproteins that are strongly expressed in the kidney where they have been originally cloned from. Previously, we have described the localization of prominin-1 in proximal tubules of the nephron. The spatial distribution of prominin-2, however, has not yet been documented in the kidney. We therefore examined the expression of this molecule along distinct tubular segments of the human and murine nephron using in situ hybridization and immunohistochemistry. Our findings indicated that human *prominin-2* transcripts and protein were confined to distal tubules of the nephron including the thick ascending limb of Henle's loop and the distal convoluted tubule, the connecting duct and to the collecting duct system. Therein, this glycoprotein was enriched at the basolateral plasma membrane of the tubular epithelial cells with exception of the thick ascending limb where it was also found in the apical domain. This is in contrast with the exclusive apical localization of prominin-1 in epithelial cells of proximal nephron tubules. The distribution of murine *prominin-2* transcripts was reminiscent of its human orthologue. In addition, a marked enrichment in the epithelium covering the papilla and in the urothelium of the renal pelvis was noted in mice. Finally, our biochemical analysis revealed that prominin-2 was released into the clinically healthy human urine as a constituent of small membrane vesicles. Collectively our data show the distribution and subcellular localization of prominin-2 within the kidney in situ and its release into the urine. Urinary detection of this protein might offer novel diagnostic approaches for studying renal diseases affecting distal segments of the nephron.

Keywords Kidney · Nephron · Collecting duct · Tubular epithelium · Basolateral membrane · Membrane vesicles · Prominin

Electronic supplementary material The online version of this article (doi:10.1007/s00418-010-0690-1) contains supplementary material, which is available to authorized users.

J. Jászai (✉) · C. A. Fargeas · P. Janich · D. Corbeil (✉)
Tissue Engineering Laboratories (BIOTEC),
DFG Research Center and Cluster of Excellence for Regenerative Therapies Dresden (CRTD), Technische Universität Dresden,
Tatzberg 47-49, 01307 Dresden, Germany
e-mail: jozsef.jaszai@biotec.tu-dresden.de

D. Corbeil
e-mail: corbeil@biotec.tu-dresden.de

L. M. Farkas · W. B. Huttner
Max-Planck-Institute of Molecular Cell Biology and Genetics,
Pfotenhauerstrasse 108, 01307 Dresden, Germany

M. Haase
Department of Pathology, Medical Faculty Carl Gustav Carus,
Technische Universität Dresden, Fetscherstrasse 74,
01307 Dresden, Germany

M. Haase
Department of Children's Surgery, Medical Faculty Carl Gustav Carus, Technische Universität Dresden, Fetscherstrasse 74,
01307 Dresden, Germany

Introduction

Prominins are evolutionarily conserved pentaspan transmembrane glycoproteins (Corbeil et al. 2001a, b; Fargeas et al. 2003a, b, 2007). Since its discovery, mammalian prominin-1 (alias CD133) has received considerable interest because of its expression by somatic stem and progenitor cells originating from different sources (Weigmann et al. 1997; Yin et al. 1997; Miraglia et al. 1997; Uchida et al. 2000; Richardson et al. 2004; Lee et al. 2005; Bussolati

et al. 2005; Sagrinati et al. 2006; Yamada et al. 2007; reviewed in Fargeas et al. 2006). Although many tissue-specific progenitor cells express prominin-1 its expression is nevertheless not limited to those with stem cell properties. Indeed, prominin-1 has been detected on the apical (luminal) side of various developing and adult epithelia found in both, mouse and human organs (Corbeil et al. 1998, 2000; Fargeas et al. 2004; Jászai et al. 2007b, 2008; Lardon et al. 2008; Karbanová et al. 2008; reviewed in Fargeas et al. 2006) including the kidney where it is expressed in proximal nephron tubules and parietal layer of the Bowman's capsule (Weigmann et al. 1997; Florek et al. 2005). Moreover, its expression is documented in non-epithelial cells such as photoreceptor and glial cells (Maw et al. 2000; Yang et al. 2008; Zacchigna et al. 2009; Corbeil et al. 2009).

Mammalian species have another prominin paralogue in their genomes. This second, as yet, less characterized member of the prominin family, shares only a moderate (≈30%) amino acid identity with prominin-1 (Corbeil et al. 2001a; Fargeas et al. 2003a). Nevertheless, both prominins interact directly with plasma membrane cholesterol within a cholesterol-dependent membrane microdomain (Röper et al. 2000; Florek et al. 2007; Janich and Corbeil 2007), and are selectively associated with plasma membrane protrusions (Weigmann et al. 1997; Fargeas et al. 2003a, 2004; Florek et al. 2007). Their physiological function is still unsolved.

Tissue expression profiling of the two *prominin* transcripts have revealed their differential expression in many organ systems with, nevertheless, some degree of intersection in the genitourinary system (Fargeas et al. 2003a; Florek et al. 2005; Jászai et al. 2008). Although the metanephros is particularly enriched in both *prominin* molecules only prominin-1 expression has been addressed at the immunohistochemical level in this organ (Weigmann et al. 1997; Florek et al. 2005). In comparison to prominin-1, the anatomical niches of prominin-2 expression are scarcely documented. While prominin-1 is expressed in both epithelial and non-epithelial cells, the tissue distribution of prominin-2 suggests that its expression is rather restricted to epithelial ones (Fargeas et al. 2003a; Jászai et al. 2007a, 2008). For instance, prominin-2 is particularly enriched in the rodent and human prostate (Zhang et al. 2002; Fargeas et al. 2003a). In the human organ, it was recently revealed as a novel marker of basal epithelial cells that are known to give rise to secretory luminal cells (Jászai et al. 2008). Beyond that, prominin-2 is detected in other segments of the male genitourinary tract including the epididymis, urothelium of the urinary bladder and glandular epithelium of the seminal vesicle (Jászai et al. 2008). Although *prominin-2* transcripts are strongly expressed in the kidney—used as source for its molecular cloning—its spatial distribution in this organ is unknown.

In the present study, we therefore investigated the expression of prominin-2 in the adult human and murine kidney as well as in newborn mice using immunohistochemistry (IHC) and non-radioactive in situ hybridization (ISH) techniques. Our data indicate among others that prominin-2 is enriched both in straight (*pars recta*; thick ascending limb of Henle's loop) and convoluted (*pars convoluta*; distal convoluted tubule) parts of the distal tubule (*tubulus distalis*) of the nephron, connecting ducts (*tubuli reunientes*) as well as in the collecting duct system (*tubuli colligentes*) of the human and mouse kidney.

Materials and methods

Tissue samples

Samples of macroscopically normal tissue from adult human kidney excised some distance (>1 cm) from nephrectomy materials derived from tumor patients were obtained from anonymous archival tissues (Department of Pathology, University of Technology Dresden). The tissues were not used for further histopathological or genetic analysis. The freshly dissected tissue was snap frozen in liquid nitrogen, and stored in a liquid nitrogen tank until use. The frozen tissue was then sectioned on a cryostat (HM560, Microm International GmbH, Walldorf, Germany) at 10 µm and sections were mounted onto SuperFrost® Plus microscope slides (Menzel-Gläser, Braunschweig, Germany). Sections were dried for 3 h at room temperature then the slides were transferred to −80°C.

Adult and newborn mouse kidney samples were obtained from NMRI strain. Mice were deeply anesthetized by a single intra-peritoneal bolus injection of Ketamine and Xylazine mixture. Animals were then trans-cardially perfused with ice-cold 4% paraformaldehyde (PFA). Kidneys were removed and post-fixed in 4% PFA for 2 h at 4°C. After cryoprotection with 30% sucrose-PBS tissue samples were embedded in OCT compound (Tissue Tek, Sakura, The Netherlands). Samples were cryosectioned at 10 µm and then mounted onto SuperFrost® Plus microscope slides (Menzel-Gläser), dried overnight at room temperature, and stored at −20°C until use.

Non-radioactive in situ hybridization

In situ hybridization on mouse and human cryosections with digoxygenin (DIG) labeled cRNA probes was performed as previously described (Jászai et al. 2007a, 2008). Briefly, serial sections were hybridized with appropriate species-specific probes at a concentration of 0.5 ng/µl for 16 h at 70°C. Stringency washes were performed at 70°C. The sections were then incubated with anti-DIG antibody

(1:4,000; Roche Molecular Biochemicals, Mannheim, Germany) for 16 h at 4°C. After several washing steps the reaction was visualized using NBT-BCIP substrate (Roche Molecular Biochemicals) giving a blue reaction product. After stopping the color reaction by several washes in PBS, sections were rinsed quickly in dH_2O and then mounted with Kaiser's Glycerol-Gelatin (Merck, Darmstadt, Germany). Images were captured using an Olympus BX61 microscope with the IPLAB software, and prepared from the digital data files using Adobe Photoshop and Illustrator software (San Jose, CA, USA).

Immunohistochemistry and lectin binding

Immunohistochemical (IHC) detection of human prominin-2 and various specific nephron-segment markers was performed on serial cryostat sections as follows. Cryosections were brought to room temperature and washed twice with PBS. Sections were incubated with 0.005% SDS in 0.2% gelatin-PBS for 30 min. The samples were then rinsed with 0.2% gelatin-PBS followed by three washing steps with 0.15% saponin/0.2% gelatin in PBS (S/G solution) for 30 min each. Sections were single- or double-labeled overnight at 4°C with mouse mAb 2024 against human prominin-2 (1:800; clone 244029; R&D Systems, Minneapolis, MN, USA) alone or in combination with polyclonal antibodies against either anti-Tamm–Horsfall protein (Uromodulin; 1:4,000; sheep; Chemicon International Inc., Billerica, MA, USA) or anti-aquaporin-2 (1:800; rabbit; Calbiochem, Darmstadt, Germany) or anti-thiazide-sensitive NaCl cotransporter (NCC; 1:2,000; rabbit; Millipore, Temecula, CA, USA) or anti-nitric oxide synthase I (NOS I; 1:100; rabbit; Cell Signaling Technology Inc.) or anti-Solute Carrier 12A1 (SLC12A1; 1:1,000; rabbit; Sigma, St. Louis, MO, USA) or anti-calbindin-D28k (1:1,000; rabbit; Chemicon), all diluted in S/G solution. In some experiments, fluorescein isothiocyanate (FITC)-conjugated *Lotus tetragonolobus* agglutinin (LTA) (1:250; Vector Laboratories, Burlingame, CA, USA) was mixed with the primary antibody. The samples were washed with 0.15% saponin in PBS followed by an extended washing step with S/G solution for 30 min. Primary antibodies were detected using appropriate fluorophore-conjugated secondary antibodies; Alexa-488 or 546-conjugated goat anti-mouse antibody, Alexa-546-conjugated donkey anti-sheep antibody and Alexa-546-conjugated goat anti-rabbit antibody (1:1,000, Molecular Probes), diluted in S/G solution. The samples were then washed in 0.15% saponin in PBS and rinsed once with PBS. In order to facilitate the identification of the tubular segments nuclei were counterstained with 4,6-diamidino-2-phenylindole (DAPI; 1 μg/ml; Molecular Probes). After washing once with PBS, slides were mounted with Mowiol 4.88 (Calbiochem). Images were captured using an Olympus BX61 compound microscope with the IPLAB software. The composite images were prepared from the digital data files using Adobe Photoshop and Illustrator software.

Combined in situ hybridization and immunohistochemistry

Combined ISH/IHC was performed as previously described (Farkas et al. 2008). Briefly, after completion of the ISH, the slides were incubated either with rabbit anti-aquaporin-2 polyclonal antibody (1:800) followed by Alexa-546-conjugated goat anti-rabbit antibody (1:1,000) or with (FITC)-conjugated LTA (1:250) as described above.

Cell culture and transfection

Chinese hamster ovary (CHO) cells were cultured in Ham's F-12 medium supplemented with 10% fetal calf serum, 100 units/ml penicillin and 100 μg/ml streptomycin under 5% CO_2. Cells were transfected with the pCMVtag-5C-hprominin-2 plasmid containing human prominin-2-coding cDNA sequence (Fargeas et al. 2003a), using Lipofect-AMINE reagent (Life Technologies, Carlsbad, CA, USA) according to the supplier's instruction. CHO cells expressing the neomycin-resistance gene were then selected by adding 600 μg/ml G418 into complete medium. Two weeks later, G418-resistant colonies were pooled and expanded. Under these conditions 10–30% of neomycin-resistant cells expressed the recombinant prominin-2.

Indirect immunofluorescence on transfected CHO cells and confocal microscopy

For immunocytochemical detection of the transgene an indirect immunofluorescence staining was performed followed by confocal microscopic analysis as described previously (Florek et al. 2005). Briefly, PFA-fixed prominin-2-transfected CHO cells were permeabilized and unspecific antibody binding was blocked by incubation with 0.2% saponin/0.2% gelatine in PBS (blocking solution) for 30 min at room temperature. They were then sequentially incubated for 30 min each with mouse mAb 2024 (1:100) and Cy2-conjugated goat anti-mouse IgG (H+L; 1:600, Jackson ImmunoResearch Labs, West Grove, PA, USA) diluted in blocking buffer. Nuclei and F-actin were labeled with DAPI (1 μg/ml) and tetramethyl-rhodamine isothiocyanate (TRITC)-conjugated phalloidin (1:500, Sigma, Saint Louis, MO, USA), respectively, during the incubation with the secondary antibody. Coverslips were rinsed and mounted in Mowiol 4.88. The samples were observed with a Zeiss 510 Meta confocal laser-scanning microscope (Jena, Germany). The confocal microscope settings were such that multipliers were

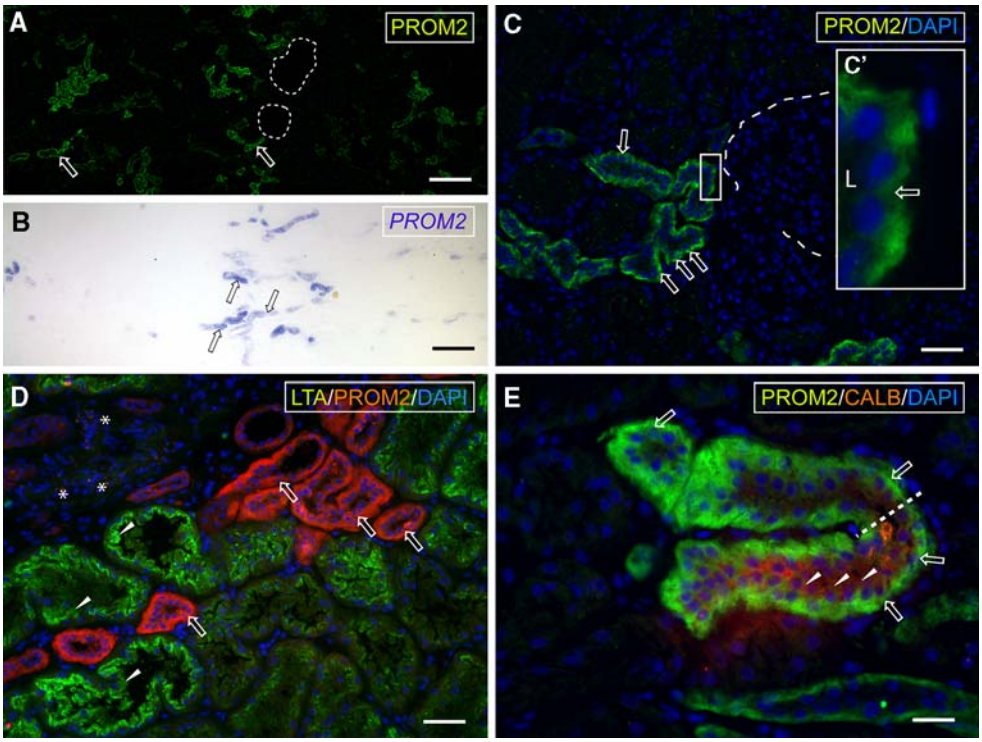

Fig. 1 Localization of human prominin-2 in the cortical labyrinth. Cryosections of human kidney were processed for either IHC (**a**, **c**–**e**) or non-radioactive ISH (**b**). **a**, **c**–**e** Sections were labeled with mAb 2024 raised against prominin-2 (*PROM2*) followed by either Alexa-488 (**a**, **c**, **c**′, **e** *green*) or -546 (**d** *red*)-conjugated goat anti-mouse secondary antibody. **d**, **e** Sections were double-labeled with either fluorophore-conjugated LTA (*LTA green*) or anti-calbindin-D28k (*CALB red*) followed by Alexa-546-conjugated goat anti-rabbit antibody, respectively. To reveal nuclear architecture of various structures, sections were counterstained with DAPI (**c**–**e** *blue*). **b** Sections were hybridized with antisense DIG-labeled *prominin-2* probe (blue reaction product). *White* (**a**, **c**–**e**) and *black* (**b**) *hollow arrows* indicate the localization prominin-2 protein and transcript, respectively, in distal convoluted tubules (**a**, **c**, **c**′, **d**) and forthcoming collecting duct (**e**). Therein, 2024 immunoreactivity is concentrated at the basolateral plasma membrane of polarized epithelial cells (*inset* **c**′, **e**). *White arrowheads* indicate LTA-positive proximal tubules (**d**) and calbindin-D28k-positive distal nephron segment, i.e. connecting tubule (**e**), respectively. Note that the intensity of calbindin-D28k labeling becomes dim on the upper part of the presented tubular segment demarcated by a *white dashed line* (**e**). *White dashed lines* indicate renal corpuscles being negative for prominin-2 (**a**, **c**). *Asterisks* background observed without primary and secondary antibodies. *L* Lumen. *Scale bars* **a**, **b** 250 μm **c**, **d** 50 μm and **e** 25 μm

within their linear range. The images shown were prepared from confocal data files using LSM 5 LIVE (Göttingen, Germany) and Adobe Photoshop and Illustrator software.

Urine and differential centrifugation

Urine was obtained from clinically healthy volunteers with informed consent and prepared as previously described (Marzesco et al. 2005). Samples were subjected to differential centrifugation steps (all done at 4°C): 5 min at 300*g*, supernatant 10 min at 1,200*g*, supernatant 30 min at 10,000*g*, supernatant 1 h at 200,000*g* and supernatant 1 h at 400,000*g*. The resulting pellets were resuspended in 40 μl SDS sample buffer. Proteins in the 400,000*g* supernatant were concentrated by methanol/chloroform (2:1) precipitation and analyzed in parallel. An equal volume (10 μl) for each protein samples was analyzed by immunoblotting for either prominin-1 or prominin-2 (see below).

SDS-PAGE and immunoblotting

Protein samples were subjected to SDS-polyacrylamide gel electrophoresis (SDS-PAGE 7.5%) and transferred poly(vinylidene difluoride) membranes (Millipore, Belford, MA, USA; pore size 0.45 μm) using a semi-dry transfer cell system (Cti, Idstein, Germany). Immunoblotting was performed as previously described (Corbeil et al. 2001b). Human prominin-1 and prominin-2 were detected using mouse mAbs 80B258 (1 μg/ml; Karbanová et al. 2008) and 2024 (1:1,000), respectively, followed by horseradish-peroxidase-conjugated secondary antibodies (Dianova, Hamburg, Germany). Antigen–antibody complexes were detected by using enhanced chemiluminescence (ECL System, Amersham Biosciences).

Anatomical terminology

To designate a particular anatomical structure, we have simultaneously used the English terminology and the

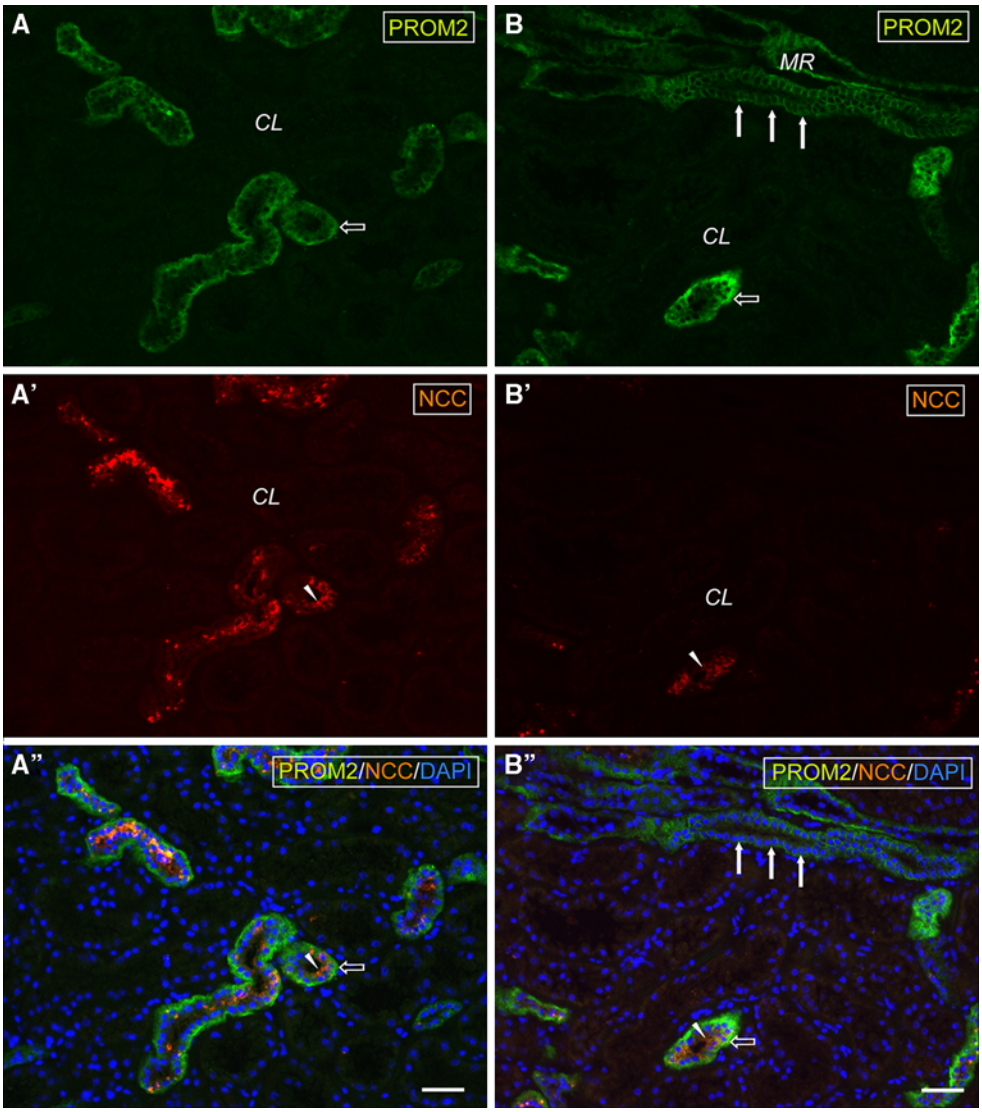

Fig. 2 Localization of prominin-2 coincides with, but not restricted to, distal convoluted tubules of the renal cortex. Cryosections of human kidney were double labeled for prominin-2 (*PROM2*) using mAb 2024 (**a**, **a**′′; **b**, **b**′′ *green*) and NCC (**a**′, **a**′′, **b**′, **b**′′ *red*) followed by appropriate fluorophore-conjugated secondary antibodies. Sections were counterstained with DAPI (**a**′′, **b**′′ *blue*). *White hollow arrow* points to prominin-2-positive cross-section profiles, which are positive for NCC within the cortical labyrinth (*CL*). *White arrows* indicate a prominin-2-positive collecting duct located in the medullary ray (*MR*), being negative for NCC. Note the regular "pearl chain-like" arrangement of the nuclei characteristic of the collecting duct system (**b**′′). *Scale bars* 50 μm

traditional Latin anatomical terminology based on Nomina Anatomica Veterinaria (NAV) and Terminologia Anatomica/Histologica (TA/TH).

Results

Localization of human prominin-2 protein and transcript in the adult kidney

To analyze the localization of prominin-2 in the adult human kidney, sections from a normal renal lobe were processed for both IHC using mAb 2024 raised against human prominin-2 and ISH using a specific human prominin-2 cRNA probe. Prior to IHC analysis on human samples, the specificity of the labeling with mAb 2024 was ascertained by indirect immunofluorescence analysis of prominin-2-transfected CHO cells (Supplemental Materials, Fig. S1). The authenticity of the immunostaining was confirmed by its dependence on the presence of human prominin-2 cDNA upon transfection of CHO cells (data not shown) and was consistent with our previous work demonstrating that mAb 2024 detected the recombinant prominin-2 on immunoblotting (Jászai et al. 2007b; see also below).

In the kidney, the 2024 immunoreactive-positive structures appeared both in the cortex and medulla (Figs. 1, 2

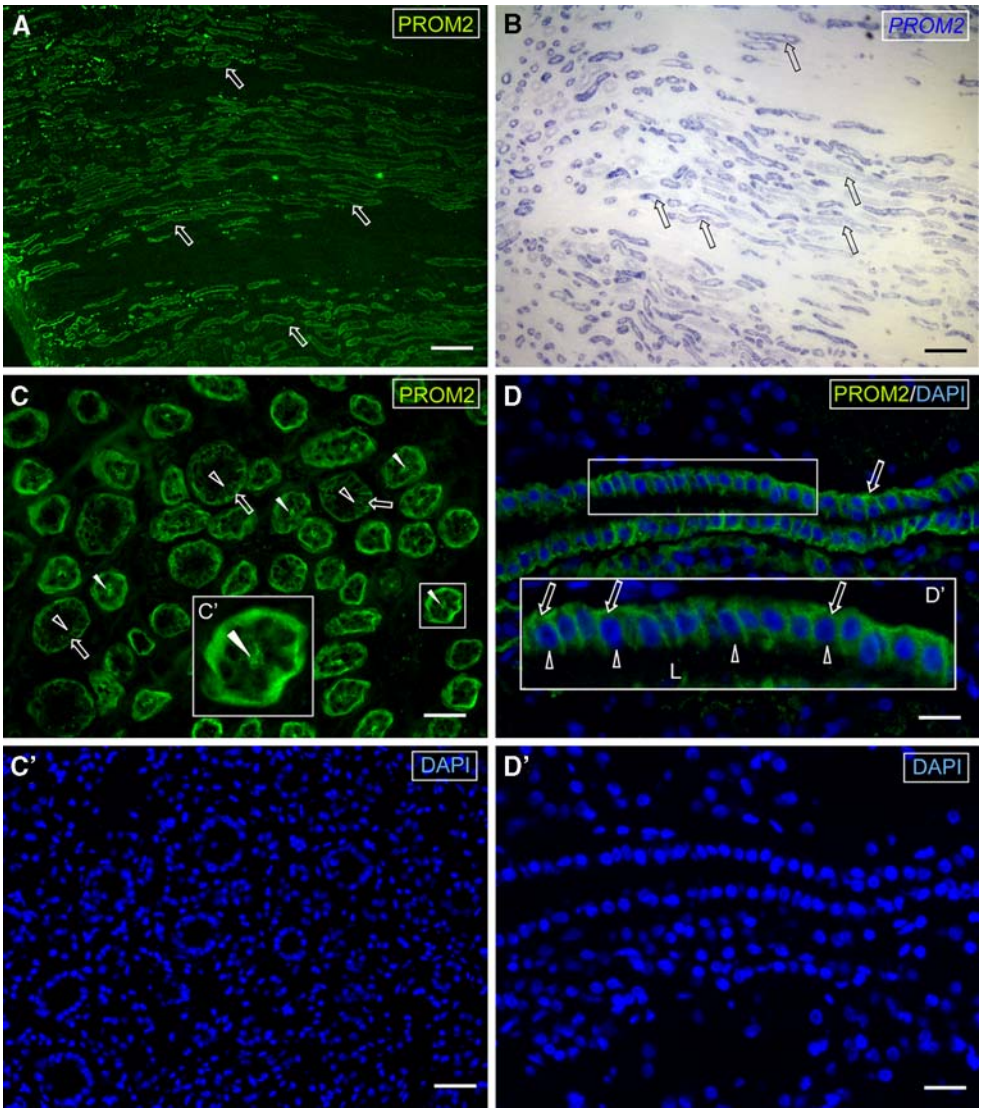

Fig. 3 Localization of human prominin-2 in the adult renal medulla. Cryosections of human kidney were processed for either IHC (**a**, **c**, **d**) or non-radioactive ISH (**b**). Sections were labeled for prominin-2 (*PROM2*) using mAb 2024 (**a**, **c**, **d** *green*) followed by appropriate fluorophore-conjugated goat anti-mouse antibody. Sections were counterstained with DAPI (**c′**, **d**–**d″** *blue*). **b** Section was hybridized with antisense DIG-labeled *prominin-2* probe (*blue*). An overview of renal medulla at the transition of inner and outer medulla (**a**, **b**), and transversal (**c**) or longitudinal (**d**) cross-section profiles of tubular segments are shown in the outer medulla. *White* (**a**) and *black* (**b**) *hollow arrows* indicate the localization of prominin-2 protein and transcript in the distal tubules present in the medullary compartment. **c**, **d** *White hollow arrows* and *arrowheads* indicate the presence or absence of 2024 immunoreactivity at the basolateral and apical plasma membrane of epithelial cells lining the collecting ducts, respectively (see enlargement in *inset* **d′**). **c** *White arrowheads* point out the 2024 immunoreactivity at the apical, in addition to basolateral, plasma membrane of cells lining tubular segments of the thick ascending limb of Henle's loop identified morphologically (see enlargement in *inset* **c′**). *L* Lumen. *Scale bars* **a**, **b** 250 μm, **c** 50 μm and **d** 25 μm

and Figs. 3, 4, 5, respectively). The immunolabeled structures in the cortex were scattered all over the cortical labyrinth (Fig. 1a; white hollow arrows; Figs. 2a, S2A; CL) and showed a parallel array in medullary rays (Figs. 2b, S2A; MR; see below). An indistinguishable expression pattern was observed by ISH confirming that the 2024 immunoreactivity was related to prominin-2 protein (Fig. 1b; black hollow arrows). The localization and morphological features of prominin-2-positive structures in the cortical labyrinth indicated that they correspond to distal segments (i.e. distal convoluted tubules and/or connecting tubules) of the nephron (see below; Fig. 1c). Renal corpuscles were negative (Fig. 1a, c; white dashed lines). To further dissect the specific localization of prominin-2, double labeling was performed with various tubular-specific markers. Proximal tubular segments were revealed by use of LTA showing strong affinity for the brush-border membrane (Laitinen et al. 1987). The fluorophore-conjugated LTA-positive proximal tubular segments (Fig. 1d; green, white arrowheads) were completely negative for mAb 2024 (Fig. 1d;

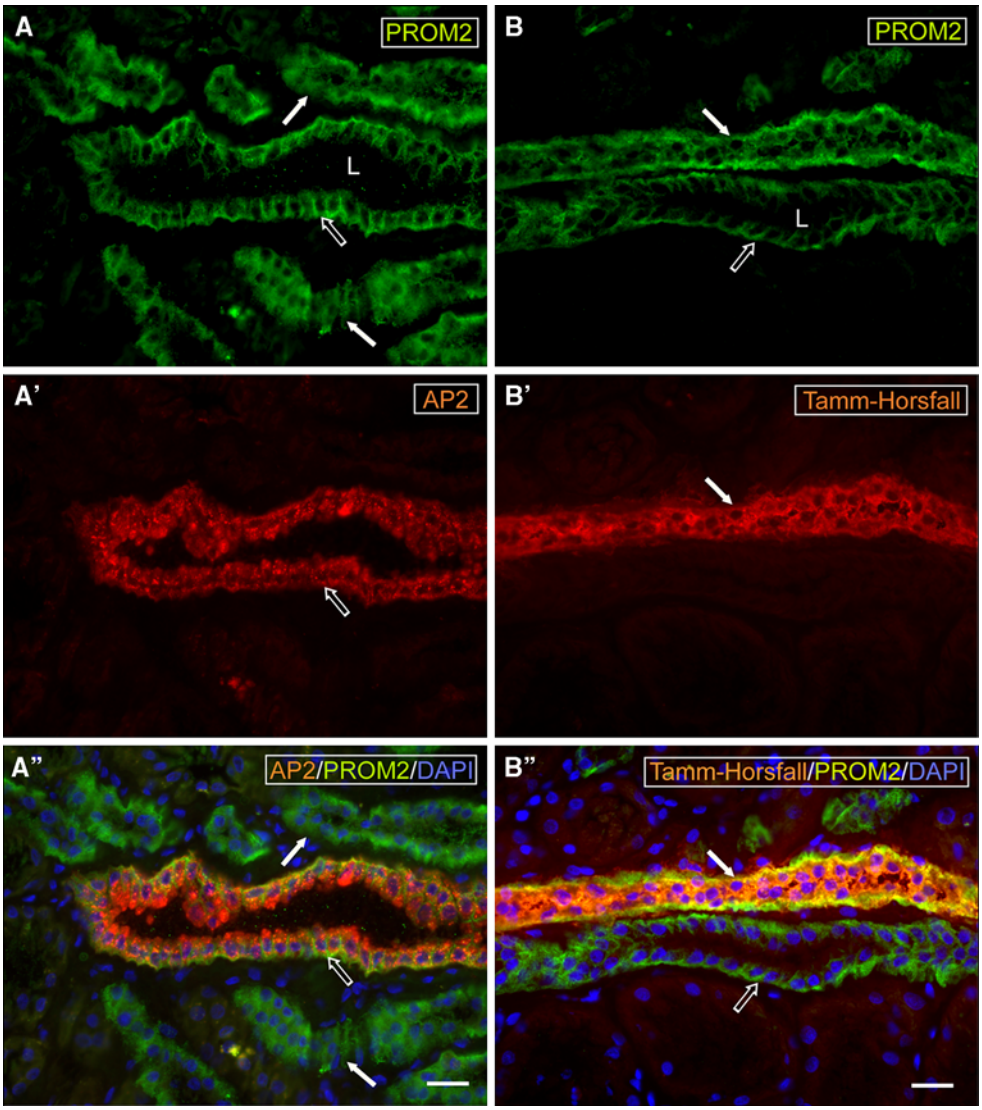

Fig. 4 Prominin-2 is associated with the collecting duct and the thick ascending limb of Henle's loop. Cryosections of human kidney were double labeled for prominin-2 (*PROM2*) using mAb 2024 (*green*) and either aquaporin-2 (*AP2*; **a**–**a**″ *red*) or Tamm–Horsfall mucoprotein (Tamm–Horsfall; **b**–**b**″ *red*) followed by appropriate fluorophore-conjugated secondary antibodies. Sections were counterstained with DAPI (**a**″, **b**″ *blue*). *White hollow arrows* indicate the collecting duct in the inner (**a**) and outer (**b**) stripe of the outer medulla. *White arrows* point to the thick ascending limb of Henle's loop. Note the regular "pearl chain-like" arrangement of the nuclei characteristic of the collecting duct system (**a**″, see also Fig. 3d–d″). *L* Lumen of the collecting duct. *Scale bars* 25 μm

red, white hollow arrows) suggesting that prominin-2 has been located in a more distal segment of the nephron. Indeed, double immunolabeling for prominin-2 and NCC, a marker of the distal convoluted tubules (Câmpean et al. 2001; Biner et al. 2002), revealed their co-localization (Fig. 2a–a″, b–b″; hollow arrows and white arrowheads, respectively). A partial co-localization of prominin-2 and calbindin-D28k, a calcium-binding protein enriched in connecting tubules (Kojima et al. 2002; El-Annan et al. 2004), was also observed suggesting the presence of prominin-2 in the distal-most segment of the nephron (Fig. 1e; hollow arrows and white arrowheads, respectively). Furthermore, the co-localization of prominin-2 either with SLC12A1 (Fig. S3A–A″; white hollow arrows and white arrowheads, respectively; see also Fig. S2) or NOS I (Fig. S4; white hollow arrow and white arrowheads, respectively) within the cortical labyrinth in the vicinity of renal corpuscles indicates its presence as well in late segments of the thick ascending limb of Henle's loop. SLC12A1 is restricted to the apical (luminal) side all along the thick ascending limb (Biner et al. 2002), while NOS I is a marker of *macula densa*, which is also found in some other cells of the thick ascending limb (Mundel et al. 1992; Bachmann et al. 1995).

At the subcellular level, the localization of 2024 immunoreactivity suggested that prominin-2 was accumulated in the basolateral plasma membrane of polarized epithelial

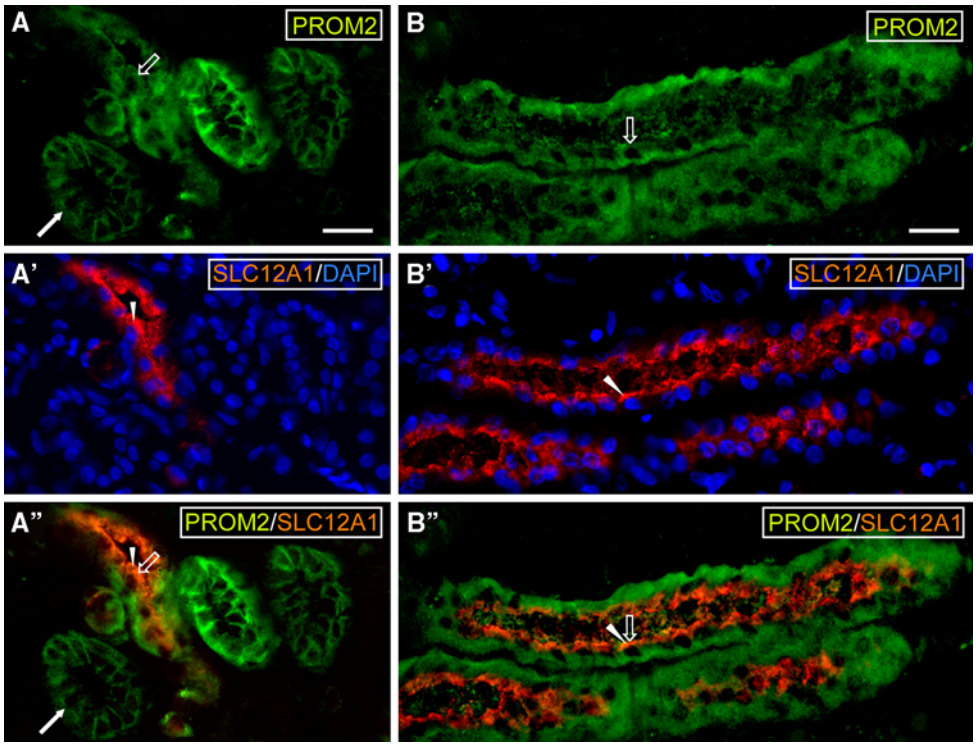

Fig. 5 Localization of prominin-2 is not restricted to the basolateral membrane in the thick ascending limb. Cryosections of human kidney were double labeled for prominin-2 (*PROM2*) using mAb 2024 (**a**, **a″**; **b**, **b″** *green*) and SLC12A1 (**a′**, **a″**; **b′**, **b″** *red*) followed by appropriate fluorophore-conjugated secondary antibodies. Sections were counterstained with DAPI (**a′**, **b′** *blue*). *White hollow arrow* indicates the prominin-2-immunoreactivity at the apical domain of tubular epithelial cells lining the lumen of the thick ascending limb of Henle's loop that are highlighted by SLC12A1 (*white arrowhead*). Note the absence of SLC12A1 immunoreactivity in collecting ducts containing a basolaterally restricted prominin-2-immunoreactivity (**a**, **a″** *white arrow*). *Scale bars* 25 μm

cells lining the distal convoluted segments while in a non-polarized fashion in late segments of the thick ascending limb of Henle's loop of the nephron located in the cortical labyrinth (Figs. 1c, e, see inset c′; S3, see inset; white hollow arrows).

In the medulla and medullary rays located in the cortex (Figs. 3, 4, 5; Figs. 2 and S2, respectively), prominin-2 was detected with a good correlation between the expression pattern of the protein and transcript (Fig. 3a, b, respectively; data not shown). IHC revealed two major—morphologically distinguishable—types of tubules that were labeled with mAb 2024, where the corresponding immunoreactivity was located in distinct subcellular compartments (Fig. 3c). In the first morphological type of tubules, the 2024 immunoreactivity was exclusively restricted to the basolateral plasma membrane of cells (Fig. 3c, d, d′; white hollow arrows) as for those found in cortical distal nephron segments (see above). These tubules, showing a characteristic pearl chain-like nuclear configuration (Fig. 3c′, d–d″; DAPI), were also immunoreactive for aquaporin-2 (Nielsen et al. 2002) indicating that they are part of the collecting duct system (Fig. 4a–a″; white hollow arrows). Importantly, not only medullary collecting ducts were labeled with mAb 2024 but also those collecting ducts that were located in medullary rays (Figs. 2b, S2A, MR; S2B). In the second type of tubules, the 2024 immunoreactivity was also observed, in addition to the basolateral membrane, at the apical plasma membrane of tubular epithelial cells (Fig. 3c, c′; white arrowheads). Given their immunoreactivity for Tamm–Horsfall protein (McKenzie and McQueen 1969; Bachmann et al. 1990), these nephron tubules were identified as the thick ascending limb of Henle's loop (Fig. 4b–b″; white arrows). Therein, the apical confinement of prominin-2 was confirmed by double immunolabeling with SLC12A1 (Figs. 5a–b″; S3B–B″). No co-localization of prominin-2 and LTA was detected indicating its exclusion from the straight portion of the proximal tubules. Thin segments of the Henle's loop were negative for prominin-2 (data not shown).

Localization of mouse *prominin-2* transcript in the adult and newborn animals

In the absence of antibody against mouse prominin-2 suitable for IHC, we investigated solely the localization of its transcript using specific mouse *prominin-2* cRNA probe. Interestingly, ISH staining of adult kidney revealed a very similar distribution pattern as observed for its human orthologue. Just like in the human kidney, the cortical labyrinth contained a scattered labeling (Fig. 6a, a′, b) and the renal medulla was intensely labeled (Fig. 6c–e) reflecting the parallel orientation of the medullar structures. Based on their localization and morphology, the major sites of *prominin-2* expression were identified as the distal tubular segments of the nephron including the thick ascending limb (Fig. 6c, d; black hollow arrows) and distal convoluted tubules (Fig. 6a, b; black hollow arrows) as well as the collecting ducts of the single renal papilla (Fig. 6e; black

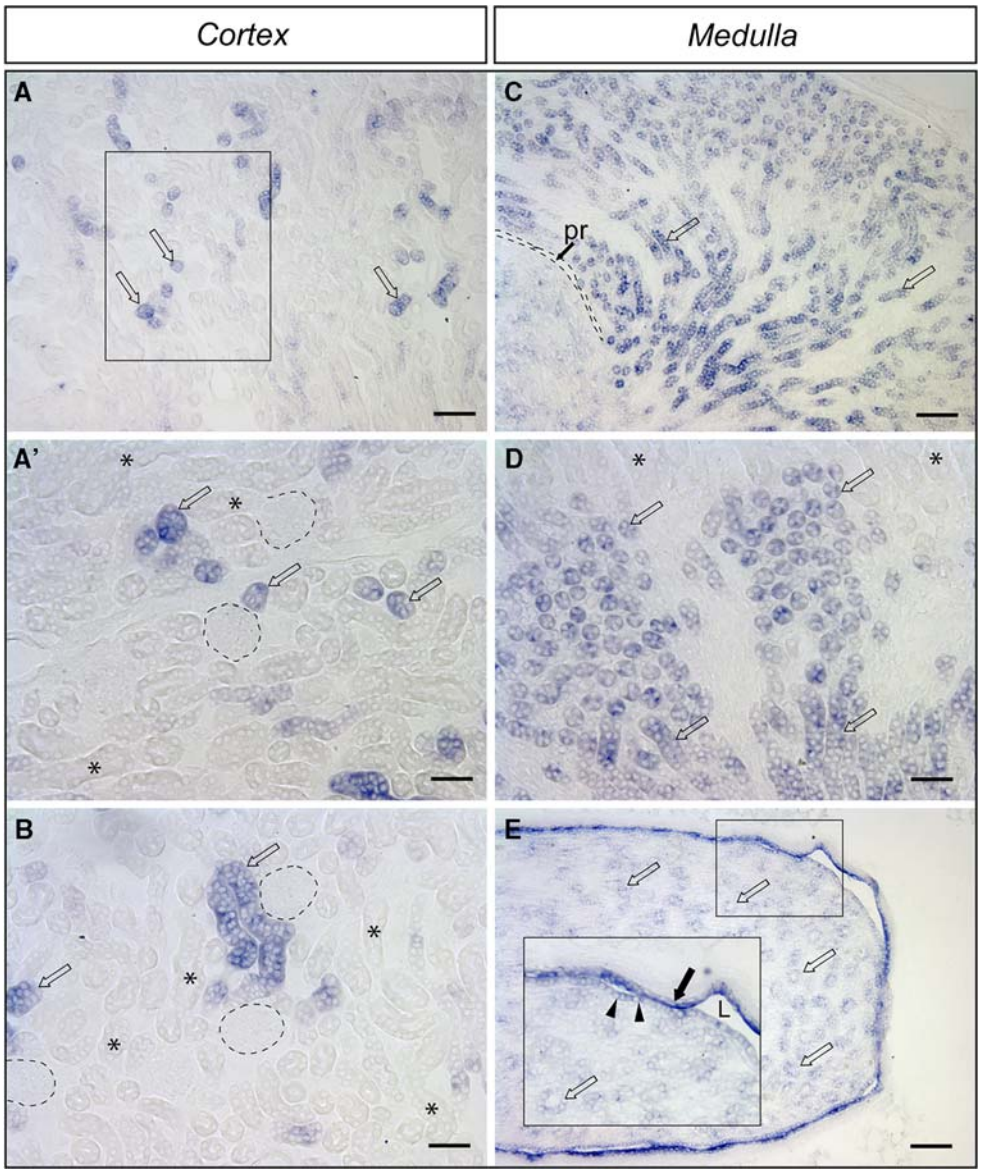

Fig. 6 Localization of mouse *prominin-2* transcript in the cortex and medulla of adult kidney. Cryosections of adult kidney were processed for non-radioactive ISH using antisense DIG-labeled *prominin-2* probe (blue reaction product). Regions from the cortical labyrinth (**a**–**b**), medulla (**c**, **d**) and papilla (**e**, **e′**) are shown. *Boxed areas* in **a** and **e** are enlarged in **a′**, **e′**, respectively. *Black hollow arrows* indicate *prominin-2*-positive distal convoluted segments (**a**, **a′**, **b**), the thick ascending limb (**c**, **d**) and collecting ducts (**e**). *Black arrowheads* and *black arrow* (**e′**) indicate epithelium covering the papilla and the urothelium of the renal pelvis, respectively, both being positive for the *prominin-2* transcript. *Asterisks* proximal tubules; *dashed lines* glomeruli; *pr* cavity of *pelvis renalis*; *L* lumen. *Scale bars* **a**, **c**, **e** 100 μm and **a′**, **b**, **d** 50 μm

hollow arrows). Renal corpuscles and proximal tubules were negative (Fig. 6a′, b, d; dashed lines and asterisks, respectively). In addition, the simple cuboidal epithelium covering the papilla and the urothelium of the renal pelvis were also labeled (Fig. 6e, e′; black arrowheads and black arrow, respectively).

A similar situation was observed in the developing neonatal murine kidney. In the cortex, the expression of *prominin-2* was detectable in the prospective distal convoluted tubules (Fig. 7a; black hollow arrows). In agreement with the adult specimen, no co-localization of *prominin-2* with fluorophore-conjugated LTA was observed indicating its exclusion from proximal tubular segments (Fig. 7a, a′; green and white dashed lines, respectively). Renal corpuscles were negative (Fig. 7a; black dashed lines). In the medulla, *prominin-2* was detectable in aquaporin-2-positive collecting tubules including ducts of the *Papilla renalis* [Bellini] (Fig. 7b, b′; black and white hollow arrows, respectively). A strong *prominin-2* labeling was also observed in the epithelium of the papilla and in the urothelium of the renal pelvis (Fig. 7b; black arrowhead and arrow, respectively).

Prominin-2 is released into the human urine

We have previously demonstrated that prominin-1 is associated with small membrane vesicles that are released into several body fluids including the human and mouse urine (Marzesco et al. 2005; Florek et al. 2007). Given the expression of prominin-2 at the apical plasma membrane of epithelial cells lining the thick ascending limb of Henle's loop (see above), we determined whether the same

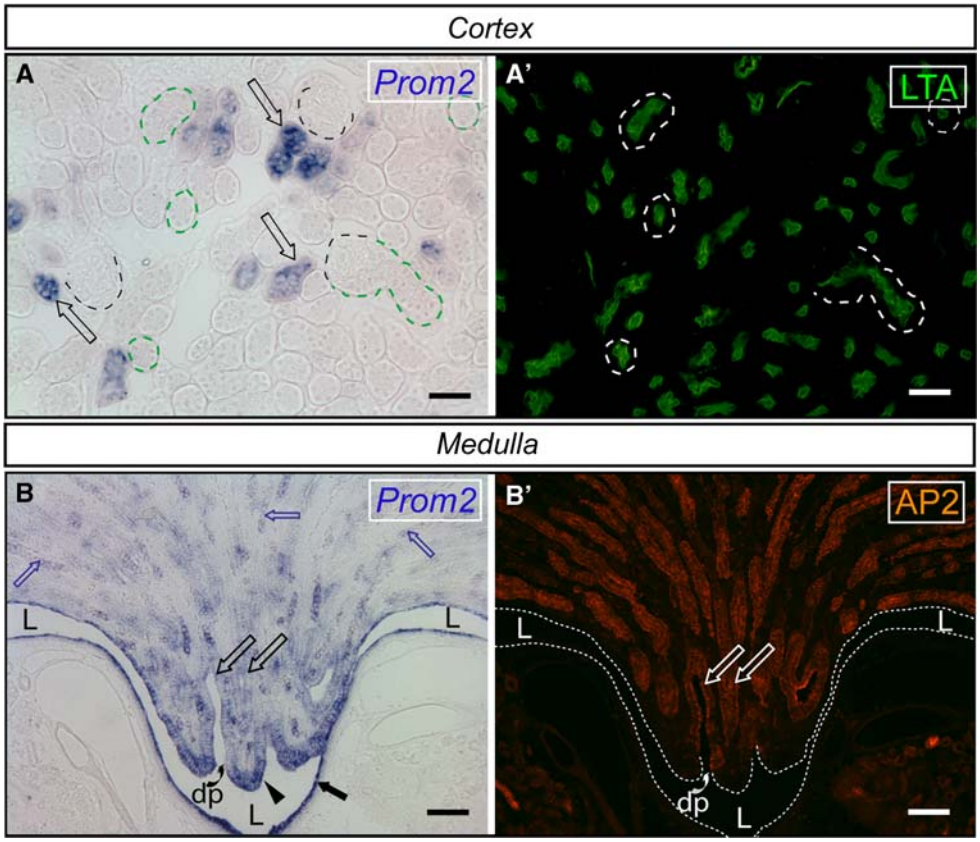

Fig. 7 Localization of mouse *prominin-2* transcripts in the developing kidney. Cryosections of kidney from newborn mice (postnatal day 0) were processed for non-radioactive ISH using antisense DIG-labeled *prominin-2* probe (*Prom2*; **a**, **b** *blue*) combined with either fluorophore-conjugated LTA (*LTA*; **a**′ *green*) or anti-aquaporin-2 antibody (*AP2*; **b**′ *red*) followed by Alexa-546-conjugated goat anti-rabbit secondary antibody labeling. Regions from the cortical labyrinth (**a**, **a**′) and renal papilla (**b**, **b**′) are shown. *Black hollow arrows* indicate *prominin-2*-positive prospective distal convoluted tubules (**a**) and *prominin-2*/aquaporin-2-positive collecting tubules (**b**; see *white hollow arrows* in **b**′). *Blue arrows* shown *prominin-2*-positive prospective loops of Henle (**b**). *Black arrowhead* and *arrow* (**b**) point out the epithelium covering the papilla and the urothelium of the renal pelvis, respectively, both being positive for the *prominin-2* transcript. Some LTA-positive proximal tubules (**a** *green*; **a**′ *white*) and glomeruli (**a** *black*) are indicated with dashed lines. *L* Lumen of the renal pelvis outlined by *dotted lines*. Dp *ductus papillaris*. *Scale bars* 100 μm

phenomenon occurred with respect to prominin-2. Examination of urine samples from clinically healthy donors by differential centrifugation followed by immunoblotting revealed the presence of prominin-2 in the 200,000*g* pellet fraction (Fig. 8, top panel, 200,000*g* pellet). By comparison to its orthologue, prominin-1, the secretion level of prominin-2 was modest (Fig. 8, top and bottom panel, respectively, 200,000*g* pellet). These data indicate that the human urine contains both prominin molecules associated with small membrane vesicles.

Discussion

In essence, we report three major observations concerning prominin-2 expression in the kidney. First, prominin-2 is confined to distal tubular segments of the nephron and collecting duct system. Second, prominin-2 is mainly expressed at the basal and lateral plasma membranes of polarized renal tubular epithelial cells. Third, prominin-2 is released into the human urine.

The anatomical compartmentalization of prominin-2 expression is distinct from those that were previously reported for prominin-1 (Weigmann et al. 1997; Florek et al. 2005). The present observation that prominin-2 is expressed in ureteric bud-derived structures of the metanephros (i.e. collecting/papillary ducts and *pelvis renalis*) is in line with our previous report of robust expression of prominin-2 in the epididymis and the seminal vesicle that are also descendants of the mesonephric duct (Jászai et al. 2008). Yet, prominin-2 expression is not confined to mesonephros-derived structures in adult kidney but extends also to the distal tubular segments of the nephron originating from the metanephric mesenchyme. This is in contrast to the expression of prominin-1 by the metanephric mesenchyme-derived proximal tubular segments and the

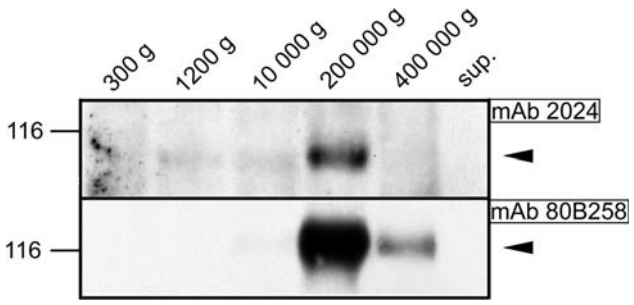

Fig. 8 Prominin-2 and prominin-1 are released into the human urine. Urine samples were subjected to differential centrifugation, and the resulting pellets were analyzed by immunoblotting for the presence of either prominin-2 or prominin-1 using mAbs 2024 and 80B258, respectively. Samples were centrifuged for 5 min at 300*g*, supernatant 10 min at 1,200*g*, supernatant 30 min at 10,000*g*, supernatant 1 h at 200,000*g* and supernatant 1 h at 400,000*g*. Proteins in the 400,000*g* supernatant (*sup*) were analyzed in parallel. *Arrowheads* indicate the corresponding prominin immunoreactive band. The position of pre-stained apparent molecular markers (in kDa) is indicated on the *left*

Bowman's capsule (Weigmann et al. 1997; Florek et al. 2005). The unique sites of expression detected for the two prominins (i.e. distinct tubular segments) are significantly different both functionally and morphologically, nevertheless, their polarized epithelial cells all have a well-elaborated system of plasma membrane protrusions (see also below). In contrast to the brush-border bearing prominin-1 expressing proximal segments, the density of apical microvillar protrusions in those distal segments that express prominin-2 is significantly lower. Instead, their epithelial cells bear a high number of membrane evaginations on their basolateral side.

A crucial observation of our study concerns the subcellular localization of prominin-2 in situ, i.e. in the natural context of renal tissue. We have previously demonstrated that prominin-1 is exclusively restricted to the apical domain of polarized epithelial cells being often concentrated at the tip of plasma membrane protrusions, e.g. microvillus (Weigmann et al. 1997; Corbeil et al. 1999, 2000) and primary cilium (Florek et al. 2007; Dubreuil et al. 2007). Both types of membrane protrusion act as donor membranes of prominin-1-containing membrane vesicles (Marzesco et al. 2005, 2009; Dubreuil et al. 2007). In contrast to prominin-1, prominin-2 is preferentially concentrated at the basolateral domain of polarized epithelial cells lining the distal nephron and collecting ducts with the notable exception of the thick ascending limb, where prominin-2 is expressed in non-polarized fashion. These results are consistent with data obtained in vitro by heterologous expression of recombinant prominin-2 in MDCK cell line (Florek et al. 2007). Collectively, these observations suggest that either prominin-2 contains both a basolateral and an apical sorting signal that compete with each other, resulting in a non-polarized distribution of the protein in certain cells or a preferential basolateral localization in others, or it is totally devoid of any sorting signal. In the latter case, its cell surface appearance might reflect its selective retention in plasma membrane protrusions (Fargeas et al. 2003a; Florek et al. 2007). In a more general note, the presence of N-linked glycans in prominin-2 (Fargeas et al. 2003a; Florek et al. 2007) indicates that carbohydrate moieties, which have been proposed to act as an apical sorting signal (Scheiffele et al. 1995; Gut et al. 1998), are insufficient to target this particular glycoprotein solely to the apical domain. Therefore, N-linked glycans should no longer be considered as a general determinant for the apical localization of membrane glycoproteins.

Finally, prominin-2 can be detected—in association with small membrane vesicles that are sedimented upon high-speed centrifugation—in the human urine as previously reported for prominin-1 (Marzesco et al. 2005). The amount of prominin-2 therein appears to be significantly lower than that of its paralogue, which might partly reflect the differences existing in their subcellular compartmentalization (i.e. apical versus basolateral). A similar phenomenon occurs in human saliva (Jászai et al. 2007b) and mouse urine (Florek et al. 2007). Thus, the high amount of prominin-1 in urine might reflect its strong expression in the brush-border membrane of the proximal tubular cells whereas the contribution of prominin-2 expressing epithelial cells is minor given that the only cells bearing this molecule on their apical (luminal) plasma membrane are those lining the thick ascending limb. It is important to note, however, that not only renal tubules express prominin-2 (this study), but also epithelia lining both the intra- and extrarenal conducting parts of the uropoëtic system including the urinary bladder (Jászai et al. 2008) making larger the spectrum of epithelia potentially releasing these vesicles. The molecular mechanism underlying the release of prominin-2-containing membrane vesicles might involve a membrane microdomain within the microvillar membrane as recently demonstrated for those carrying prominin-1 (Marzesco et al. 2009). Although, the physiological relevance of the prominin-containing membrane vesicles found in the urine and other body fluids is unknown, they might offer a valuable biological tool for diagnostic purposes of certain solid cancers, e.g. kidney cancer (Florek et al. 2005), as recently proposed for central nervous system diseases (Huttner et al. 2008). Likewise, analyzing the prominin content, in conjunction with other constituents of the urine, might be clinically useful for monitoring functional recovery of the kidney upon tissue engineering/cell replacement therapies.

Acknowledgments We thank Sylvi Graupner and Suzanne Manthey for the skillful assistance for preparing the cryosection samples.

W. B. H. and D. C. were supported by the Deutsche Forschungsgemeinschaft (SFB/TR 83 #6, SFB 655 A2 (W. B. H.) and B3 (D. C.)).

References

Bachmann S, Metzger R, Bunnemann B (1990) Tamm-Horsfall protein-mRNA synthesis is localized to the thick ascending limb of Henle's loop in rat kidney. Histochemistry 94:517–523

Bachmann S, Bosse HM, Mundel P (1995) Topography of nitric oxide synthesis by localizing constitutive NO synthases in mammalian kidney. Am J Physiol 268:F885–F898

Biner HL, Arpin-Bott MP, Loffing J, Wang X, Knepper M, Hebert SC, Kaissling B (2002) Human cortical distal nephron: distribution of electrolyte and water transport pathways. J Am Soc Nephrol 13:836–847

Bussolati B, Bruno S, Grange C, Buttiglieri S, Deregibus MC, Cantino D, Camussi G (2005) Isolation of renal progenitor cells from adult human kidney. Am J Pathol 166:545–555

Câmpean V, Kricke J, Ellison D, Luft FC, Bachmann S (2001) Localization of thiazide-sensitive Na(+)-Cl(−) cotransport and associated gene products in mouse DCT. Am J Physiol Renal Physiol 281:F1028–F1035

Corbeil D, Röper K, Weigmann A, Huttner WB (1998) AC133 hematopoietic stem cell antigen: human homologue of mouse kidney prominin or distinct member of a novel protein family? Blood 91:2625–2626

Corbeil D, Röper K, Hannah MJ, Hellwig A, Huttner WB (1999) Selective localization of the polytopic membrane protein prominin in microvilli of epithelial cells—a combination of apical sorting and retention in plasma membrane protrusions. J Cell Sci 112:1023–1033

Corbeil D, Röper K, Hellwig A, Tavian M, Miraglia S, Watt SM, Simmons PJ, Peault B, Buck DW, Huttner WB (2000) The human AC133 hematopoietic stem cell antigen is also expressed in epithelial cells and targeted to plasma membrane protrusions. J Biol Chem 275:5512–5520

Corbeil D, Röper K, Fargeas CA, Joester A, Huttner WB (2001a) Prominin: a story of cholesterol, plasma membrane protrusions and human pathology. Traffic 2:82–91

Corbeil D, Fargeas CA, Huttner WB (2001b) Rat prominin, like its mouse and human orthologues, is a pentaspan membrane glycoprotein. Biochem Biophys Res Commun 4:939–944

Corbeil D, Joester A, Fargeas CA, Jászai J, Garwood J, Werner HB, Huttner WB (2009) Expression of distinct splice variants of the stem cell marker prominin-1 (CD133) in glial cells. Glia 57:860–874

Dubreuil V, Marzesco A-M, Corbeil D, Huttner WB, Wilsch-Bräuninger M (2007) Midbody and primary cilium of neural progenitors release extracellular membrane particles enriched in the stem cell marker prominin-1. J Cell Biol 176:483–495

El-Annan J, Brown D, Breton S et al (2004) Differential expression and targeting of endogenous Arf1 and Arf6 small GTPases in kidney epithelial cells in situ. Am J Physiol Cell Physiol 286:C768–C778

Fargeas CA, Florek M, Huttner WB, Corbeil D (2003a) Characterization of prominin-2, a new member of the prominin family of pentaspan membrane glycoproteins. J Biol Chem 278:8586–8596

Fargeas CA, Corbeil D, Huttner WB (2003b) AC133 antigen, CD133, prominin-1, prominin-2. etc.: prominin family gene products in need of a rational nomenclature. Stem Cells 21:506–508

Fargeas CA, Joester A, Missol-Kolka E, Hellwig A, Huttner WB, Corbeil D (2004) Identification of novel prominin-1/CD133 splice variants with alternative C-termini and their expression in epididymis and testis. J Cell Sci 117:4301–4311

Fargeas CA, Fonseca A-V, Huttner WB, Corbeil D (2006) Prominin-1 (CD133)—from progenitor cells to human diseases. Future Lipidol 1:213–225

Fargeas CA, Huttner WB, Corbeil D (2007) Nomenclature of prominin-1 (CD133) splice variants - an update. Tissue Antigens 69:602–606

Farkas LM, Haffner C, Giger T, Khaitovich P, Nowick K, Birchmeier C, Pääbo S, Huttner WB (2008) Insulinoma-associated 1 has a panneurogenic role and promotes the generation and expansion of basal progenitors in the developing mouse neocortex. Neuron 60:40–55

Florek M, Haase M, Marzesco AM, Freund D, Ehninger G, Huttner WB, Corbeil D (2005) Prominin-1/CD133, a neural and hematopoietic stem cell marker, is expressed in adult human differentiated cells and certain types of kidney cancer. Cell Tissue Res 319:15–26

Florek M, Bauer N, Janich P, Wilsch-Bräuninger M, Fargeas CA, Marzesco A-M, Ehninger G, Thiele C, Huttner WB, Corbeil D (2007) Prominin-2 is a cholesterol-binding protein associated with apical and basolateral plasmalemmal protrusions in polarized epithelial cells and released into urine. Cell Tissue Res 328:31–47

Gut A, Kappeler F, Hyka N, Balda MS, Hauri HP, Matter K (1998) Carbohydrate-mediated Golgi to cell surface transport and apical targeting of membrane proteins. EMBO J 17:1919–1929

Huttner HB, Janich P, Köhrmann M, Jászai J, Siebzehnrubl F, Blümcke I, Suttorp M, Gahr M, Kuhnt D, Nimsky C, Krex D, Schackert G, Löwenbrück K, Reichmann H, Jüttler E, Hacke W, Schellinger P, Schwab S, Wilsch-Bräuninger M, Marzesco A-M, Corbeil D (2008) The stem cell marker prominin-1/CD133 on membrane particles in human cerebrospinal fluid offers novel approaches for studying CNS disease. Stem Cells 26:698–705

Janich P, Corbeil D (2007) GM_1 and GM_3 gangliosides highlight distinct lipid microdomains within the apical domain of epithelial cells. FEBS Lett 581:1783–1787

Jászai J, Fargeas CA, Florek M, Huttner WB, Corbeil D (2007a) Focus on molecules: prominin-1 (CD133). Exp Eye Res 85:585–586

Jászai J, Janich P, Farkas LM, Fargeas CA, Huttner WB, Corbeil D (2007b) Differential expression of prominin-1 (CD133) and prominin-2 in major cephalic exocrine glands of adult mice. Histochem Cell Biol 128:409–419

Jászai J, Fargeas CA, Haase M, Farkas LM, Huttner WB, Corbeil D (2008) Robust expression of prominin-2 all along the adult male reproductive system and urinary bladder. Histochem Cell Biol 130:749–759

Karbanová J, Missol-Kolka E, Fonseca AV, Lorra C, Janich P, Hollerová H, Jászai J, Ehrmann J, Kolár Z, Liebers C, Arl S, Subrtová D, Freund D, Mokry J, Huttner WB, Corbeil D (2008) The stem cell marker CD133 (prominin-1) is expressed in various human glandular epithelia. J Histochem Cytochem 56:977–993

Kojima R, Sekine T, Kawachi M et al (2002) Immunolocalization of multispecific organic anion transporters, OAT1, OAT2, and OAT3, in rat kidney. J Am Soc Nephrol 13:848–857

Laitinen L, Virtanen I, Saxén L (1987) Changes in the glycosylation pattern during embryonic development of mouse kidney as revealed with lectin conjugates. J Histochem Cytochem 35:55–65

Lardon J, Corbeil D, Huttner WB, Ling Z, Bouwens L (2008) Stem cell marker prominin-1/AC133 is expressed in duct cells of the adult human pancreas. Pancreas 36:e1–e6

Lee A, Kessler JD, Read TA, Kaiser C, Corbeil D, Huttner WB, Johnson JE, Wechsler-Reya RJ (2005) Isolation of neural stem cells from the postnatal cerebellum. Nat Neurosci 8:723–729

Marzesco A-M, Janich P, Wilsch-Bräuninger M, Dubreuil V, Langenfeld K, Corbeil D, Huttner WB (2005) Release of extracellular membrane particles carrying the stem cell marker prominin-1 (CD133) from neural progenitors and other epithelial cells. J Cell Sci 118:2849–2858

Marzesco A-M, Wilsch-Bräuninger M, Dubreuil V, Janich P, Langenfeld K, Thiele C, Huttner WB, Corbeil D (2009) Release of extracellular membrane vesicles from microvilli of epithelial cells is enhanced by depleting membrane cholesterol. FEBS Lett 583:897–902

Maw MA, Corbeil D, Koch J, Hellwig A, Wilson-Wheeler JC, Bridges RJ, Kumaramanickavel G, John S, Nancarrow D, Röper K, Weigmann A, Huttner WB, Denton MJ (2000) A frameshift mutation in prominin (mouse)-like 1 causes human retinal degeneration. Hum Mol Genet 9:27–34

McKenzie JK, McQueen EG (1969) Immunofluorescent localization of Tamm-Horsfall mucoprotein in human kidney. J Clin Pathol 22:334–339

Miraglia S, Godfrey W, Yin AH, Atkins K, Warnke R, Holden JT, Bray RA, Waller EK, Buck DW (1997) A novel five-transmembrane hematopoietic stem cell antigen: isolation, characterization, and molecular cloning. Blood 90:5013–5021

Mundel P, Bachmann S, Bader M, Fischer A, Kummer W, Mayer B, Kriz W (1992) Expression of nitric oxide synthase in kidney macula densa cells. Kidney Int 42:1017–1019

Nielsen S, Frøkiaer J, Marples D, Kwon TH, Agre P, Knepper MA (2002) Aquaporins in the kidney: from molecules to medicine. Physiol Rev 82:205–244

Richardson GD, Robson CN, Lang SH, Neal DE, Maitland NJ, Collins AT (2004) CD133, a novel marker for human prostatic epithelial stem cells. J Cell Sci 117:3539–3545

Röper K, Corbeil D, Huttner WB (2000) Retention of prominin in microvilli reveals distinct cholesterol-based lipid micro-domains in the apical plasma membrane. Nat Cell Biol 2:582–592

Sagrinati C, Netti GS, Mazzinghi B, Lazzeri E, Liotta F, Frosali F, Ronconi E, Meini C, Gacci M, Squecco R, Carini M, Gesualdo L, Francini F, Maggi E, Annunziato F, Lasagni L, Serio M, Romagnani S, Romagnani P (2006) Isolation and characterization of multipotent progenitor cells from the Bowman's capsule of adult human kidneys. J Am Soc Nephrol 17:2443–2456

Scheiffele P, Peranen J, Simons K (1995) N-glycans as apical sorting signals in epithelial cells. Nature 378:96–98

Uchida N, Buck DW, He D, Reitsma MJ, Masek M, Phan TV, Tsukamoto AS, Gage FH, Weissman IL (2000) Direct isolation of human central nervous system stem cells. Proc Natl Acad Sci USA 97:14720–14725

Weigmann A, Corbeil D, Hellwig A, Huttner WB (1997) Prominin, a novel microvilli-specific polytopic membrane protein of the apical surface of epithelial cells, is targeted to plasmalemmal protrusions of non-epithelial cells. Proc Natl Acad Sci USA 94:12425–12430

Yamada Y, Yokoyama S, Wang XD, Fukuda N, Takakura N (2007) Cardiac stem cells in brown adipose tissue express CD133 and induce bone marrow nonhematopoietic cells to differentiate into cardiomyocytes. Stem Cells 25:1326–1333

Yang Z, Chen Y, Lillo C, Chien J, Michaelides M, Klein M, Howes KA, Li Y, Kaminoh Y, Chen H, Zhao C, Chen Y, Al-Sheikh YT, Karan G, Corbeil D, Escher P, Kamaya S, Li C, Johnson S, Frederick JM, Zhao Y, Wang C, Cameron DJ, Huttner WB, Schorderet DF, Munier FL, Moore AT, Birch DG, Baehr W, Hunt DM, Williams DS, Zhang K (2008) Mutant prominin-1 found in patients with macular degeneration disrupts photoreceptor disk morphogenesis in mice. J Clin Invest 118:2908–2916

Yin AH, Miraglia S, Zanjani ED, Almeida-Porada G, Ogawa M, Leary AG, Olweus J, Kearney J, Buck DW (1997) AC133, a novel marker for human hematopoietic stem and progenitor cells. Blood 90:5002–5012

Zacchigna S, Oh H, Wilsch-Bräuninger M, Missol-Kolka E, Jászai J, Jansen S, Tanimoto N, Tonagel F, Seeliger M, Huttner WB, Corbeil D, Dewerchin M, Vinckier S, Moons L, Carmeliet P (2009) Loss of cholesterol-binding protein prominin-1/CD133 causes disk dysmorphogenesis and photoreceptor degeneration. J Neurosci 29:2297–2308

Zhang Q, Haleem R, Cai X, Wang Z (2002) Identification and characterization of a novel testosterone-regulated prominin-like gene in the rat ventral prostate. Endocrinology 143:4788–4796